AGU PUBLICATIONS

Geophysical Research Letters

RESEARCH LETTER
10.1002/2015GL064431

Key Points:
- Natural pH variability is larger than expected due to pCO_2 changes
- Ocean circulation and biogeochemistry drive pH

Supporting Information:
- Supporting Information S1

Correspondence to:
N. F. Goodkin,
NATHALIE@ntu.edu.sg

Citation:
Goodkin, N. F., B.-S. Wang, C.-F. You, K. A. Hughen, N. Grumet-Prouty, N. R. Bates, and S. C. Doney (2015), Ocean circulation and biogeochemistry moderate interannual and decadal surface water pH changes in the Sargasso Sea, *Geophys. Res. Lett.*, *42*, 4931–4939, doi:10.1002/2015GL064431.

Received 6 MAY 2015
Accepted 3 JUN 2015
Accepted article online 5 JUN 2015
Published online 25 JUN 2015

Ocean circulation and biogeochemistry moderate interannual and decadal surface water pH changes in the Sargasso Sea

Nathalie F. Goodkin[1,2], Bo-Shian Wang[3,4], Chen-Feng You[3], Konrad A. Hughen[5], Nancy Grumet-Prouty[5,6], Nicholas R. Bates[7], and Scott C. Doney[5]

[1]Asian School of the Environment, Nanyang Technological University, Singapore, [2]Earth Observatory of Singapore, Singapore, [3]Department of Earth Sciences, National Cheng Kung University, Tainan, Taiwan, [4]Now at Academia Sinica, Taipei, Taiwan, [5]Woods Hole Oceanographic Institution, Woods Hole, Massachusetts, USA, [6]Now at United States Geological Survey, Menlo Park, California, USA, [7]Bermuda Institute of Ocean Sciences, St. George's, Bermuda

Abstract The oceans absorb anthropogenic CO_2 from the atmosphere, lowering surface ocean pH, a concern for calcifying marine organisms. The impact of ocean acidification is challenging to predict as each species appears to respond differently and because our knowledge of natural changes to ocean pH is limited in both time and space. Here we reconstruct 222 years of biennial seawater pH variability in the Sargasso Sea from a brain coral, *Diploria labyrinthiformis*. Using hydrographic data from the Bermuda Atlantic Time-series Study and the coral-derived pH record, we are able to differentiate pH changes due to surface temperature versus those from ocean circulation and biogeochemical changes. We find that ocean pH does not simply reflect atmospheric CO_2 trends but rather that circulation/biogeochemical changes account for >90% of pH variability in the Sargasso Sea and more variability in the last century than would be predicted from anthropogenic uptake of CO_2 alone.

1. Introduction

The release of carbon dioxide (CO_2) through burning of fossil fuels, industrialization, and alteration of landmass changes since the Industrial Revolution (late 1800s) has led to a rapid rise in atmospheric CO_2 [*Etheridge et al.*, 1996; *Keeling et al.*, 1976] over the last century and absorption of anthropogenically derived CO_2 in the global ocean. Current assessments indicate that approximately 25% of anthropogenic CO_2 has been being absorbed into the ocean [*Fung et al.*, 2005; *Le Quere et al.*, 2009; *Quay et al.*, 2003; *Sabine et al.*, 2004]. As the ocean absorbs CO_2, its buffering capacity is lessened, and predictions suggest that surface ocean pH could drop by 0.2–0.3 units during the 21st century, thus lowering calcium carbonate ($CaCO_3$) saturation levels for biogenically important minerals such as calcite and aragonite [*Orr et al.*, 2005]. Ultimately, such chemical changes to the ocean could challenge the direct ability of marine organisms to calcify and could indirectly alter many other biogeochemical processes to threaten global marine ecosystems [*Doney et al.*, 2009].

The natural variability of seawater pH is poorly constrained in many marine ecosystems due to limited observations. For coral reefs, previous research on the Great Barrier Reef (GBR) using coral paleo-pH reconstructions has shown that on decadal time scales, reef systems can experience pH changes of greater than 0.2 pH units, significantly larger than the current estimates of changes due to anthropogenic CO_2 alone [*Pelejero et al.*, 2005]. Changes in the GBR pH were attributed to climate forcing that altered the rates of currents flushing the lagoonal reef and thus were primarily a result of seawater CO_2-carbonate chemistry changes due to reef geometry rather than atmospheric chemistry [*Pelejero et al.*, 2005]. Thus, in addition to gradual changes in ocean chemistry imparted by anthropogenic CO_2, a suite of synergistic and feedback physicobiogochemical mechanisms can mitigate or amplify ocean acidification effects [e.g., *Andersson et al.*, 2014; *Bates et al.*, 2010].

In order to improve our understanding of seawater pH and its impact on marine taxa and ecosystems, we need to increase the temporal and spatial coverage of both instrumental and paleo-pH records. The imperative for this approach is to better constrain natural variability of seawater pH and assess the ability of calcifiers to maintain function in changing waters. A refined approach is to use boron (B) isotopes

($^{11}B/^{10}B$) in biogenic $CaCO_3$ as a key proxy for investigating past ocean water pH. The proxy is based on the premise that dissolved seawater B has a constant $\delta^{11}B$ of 39.5‰ and that the relative concentration and isotopic composition of the two B species ($B(OH)_3$ and $B(OH)_4^-$) are kinetically dependent on seawater pH [*Klochko et al*., 2006]. Marine calcifiers are presumed to uptake predominantly $B(OH)_4^-$ into their skeletal architecture, thus reflecting the $\delta^{11}B$ of dissolved $B(OH)_4^-$ from which the pH can be calculated [*Hemming and Hanson*, 1992]. Concerns regarding the interpretation of this proxy in corals have focused on the fact that corals calcify in an internal microenvironment (i.e., in the calicoblastic fluids at the site of calcification) that is chemically modified to induce aragonite precipitation via up-regulation of the fluid's pH. Thus, the coral skeletons potentially reflect the pH of the fluid at the calcifying site rather than the surrounding seawater, making thermodynamic reconstructions of seawater pH challenging without instrumental pH records against which to calibrate the offset imparted by internal physiological and biogeochemical processes [*Anagnostou et al*., 2012; *McCulloch et al*., 2012]. Previous research has thus focused either on coral culture experiments, which allow for the calibration of each species' $CaCO_3$ $\delta^{11}B$ to known pH [*Hönisch et al*., 2004; *Krief et al*., 2010; *Reynaud et al*., 2004], or on adjusting the thermodynamic fractionation factor (α) to 20.0‰ from 27.2‰ [*Klochko et al*., 2006], which attempts to correct for the coral up-regulated pH [*Hönisch et al*., 2007].

Here we reconstruct 222 years of biennial pH from a coral colony collected on the south shore of Bermuda and, compare and calibrate the record to seawater CO_2-carbonate chemistry collected nearby at the Bermuda Atlantic Time-series Study (BATS) site. This coral was previously found to reflect conditions more similar to the open ocean than to the northern Bermuda lagoonal reef environment [*Goodkin et al*., 2008a; *Goodkin et al*., 2012]. We use this coral pH record to investigate the time-frequency variability of pH in the Sargasso Sea and the possible drivers of these changes.

2. Oceanographic Setting

Bermuda is located in the northwestern Atlantic Basin (32°N, 64°W) in a region sensitive to many North Atlantic coupled ocean-atmospheric processes. Three key North Atlantic climate modes impacting the ocean circulation and biogeochemistry of the region are the North Atlantic Oscillation (NAO), the tropical Atlantic variability (TAV) and the Atlantic meridional overturning circulation (AMOC) as described by *Marshall et al*. [2001].

The NAO is measured as the oscillation of surface atmospheric pressure between Iceland (65°N, 23°W) and the Açores (38°N, 26°W). The NAO is the dominant mode of winter pressure variability over the North Atlantic and is viewed as largely driving climate variability in the region [*Hurrell*, 1995; *Hurrell et al*., 2003]. In a positive NAO index (NAOI), both the low-pressure zone over Iceland and the high-pressure zone over the Açores are intensified, resulting in stronger winter storms crossing the Atlantic along more northerly paths, deepening the surface ocean mixed layer and increasing the production of subtropical mode (or 18°C) water [*Bates*, 2012]. Low-frequency (decadal and longer) variability of the NAO has been shown to be increasing by a factor of two since the 1900s with long-term impacts on ocean circulation and water mass advection [*Goodkin et al*., 2008a; *Visbeck et al*., 1998] and seawater CO_2-carbonate chemistry [e.g., *Levine et al*., 2011; *Bates*, 2012].

The TAV is loosely defined as the covariation of the sea surface temperature (SST) gradient across the equator (ΔT_{eq}) and the weakening/strengthening of trade winds. TAV varies primarily as a result of the NAO that sets up a regional tripole SST spatial pattern leading to cool (warm) SSTs during positive (negative) NAO in the tropics and the opposite pattern at Bermuda [*Hurrell*, 1995]. In addition, TAV is correlated to the (El Nino) Southern Oscillation Index (SOI), which is measured as the monthly sea level pressure difference between Tahiti and Darwin [*Ropelewski and Jones*, 1987; *Trenberth*, 1984; *Trenberth and Hoar*, 1996]. In a positive SOI year, trade winds slacken globally leading to generally increased SSTs in the tropical Atlantic and decreased SSTs at Bermuda [*Alexander et al*., 2001] with synergistic changes in primary production [*Bates*, 2001].

The AMOC is the basin-scale thermohaline circulation of water from the tropics to the northern Atlantic seas where they are subsequently down welled. Rates of AMOC circulation are known to change primarily on decadal and subdecadal timescales resulting in changes to the buoyancy of water masses in the North Atlantic [*Bjerknes*, 1964]. A slowdown in the AMOC is necessarily connected to a slowing of the Gulf Stream

and the advection of water around the Atlantic basin. While there is no long-term record of the AMOC, fluctuations in the Atlantic Multidecadal Oscillation (AMO), based on calculated basin-averaged SST anomalies for the North Atlantic, are generally accepted to be due in large part to fluctuations in the AMOC [*Enfield et al.*, 2001; *Kaplan et al.*, 1998].

3. Materials and Methods

3.1. Coral Collection and Subsampling

A multicentury old *Diploria labyrinthiformis* colony was collected from the south shore of Bermuda off John Smith's Bay (32°19'N, 64°43'W) in 2000. The coral was sectioned along the primary growth axis, sonicated in deionized water, dried at 50°C, and X-rayed at Falmouth Hospital, Massachusetts (film focus = 100 cm, exposure = 0.2 s, voltage = 50 kV, and current = 16 mA). Continuous 2 year sections delineated by high-low density bands (approximately November to October), spanning the period of 1774–1996, were removed from the coral slab with a diamond wire band saw and crushed using an agate mortar and pestle as previously described [*Goodkin et al.*, 2005; *Prouty et al.*, 2013]. Samples include dominantly thecal material, and less dense smaller fraction material will be lost in cleaning as described below. Two year increments were chosen as a balance between samples size, resolution, and analytical costs.

3.2. Coral Cleaning and Isotopic Measurement

Coral subsamples were cleaned in class 10 laminar flow benches at the Class 1000 clean room of the Isotope Geochemistry Laboratory (IGL), National Cheng Kung University, Taiwan. Coral powder was soaked overnight in deionized water, and then the supernatant was removed. Samples were washed five times by vigorously rinsing in deionized water, sonicating, and centrifuging (3200 rpm, 10 min). Organic matter was removed by soaking samples in 10% sodium hypochlorite (NaOCl) and then rinsed, sonicated, and centrifuged an additional 5 times. Coral powders were then rinsed 5 times in 7.5 mM HNO_3, followed by five additional deionized water rinses. The supernatant was removed, and the cleaned coral powder was fully dissolved in 100 μL of 1 M HNO_3. Purification of samples by microsublimation was performed following [*Wang et al.*, 2010] and samples were diluted to 20 ppb B.

$\delta^{11}B$ measurements were made on a Thermo Fisher Scientific Neptune inductively coupled plasma mass spectrometer at IGL. Samples were bracketed with National Institute of Standards and Technology Standard Reference Material (NIST SRM) 951 to correct for mass bias, and long-term precision of the analysis was ± 0.27‰ (2 standard deviation, $n = 88$). Sample $\delta^{11}B$ was calculated as the deviation per mil from NIST SRM 951.

3.3. Hydrographic Data

We utilize ocean field data from August 1983 to October 1999, including seawater pH (pH units), dissolved inorganic carbon (DIC, μmol kg_{sw}^{-1}), total alkalinity (TA, μmol kg_{sw}^{-1}), sea surface temperature (SST, °C), and sea surface salinity (SSS) [*Bates et al.*, 2012]. Data were collected from Hydrostation S prior to 1988 and at BATS since 1988. All reported data are from surface samples, and data between the two locations are not statistically different [*Bates et al.*, 2012]. Seawater parameters were averaged from November to October over 2 year periods to match coral subsampling. Surface TA was regressed against DIC to establish a long-term relationship such that

$$\mathrm{TA} = m_0 + m_1 \times \mathrm{DIC} \quad (1)$$

where m_0 is 1290.4 μmol TA kg_{sw}^{-1}, m_1 is 0.54 μmol TA kg_{sw}^{-1} (μmol DIC $kg_{sw}^{-1})^{-1}$, $r^2 = 0.65$, $p = 0.03$, and $n = 7$. While SSS describes more TA variability than does DIC (supporting information Figure S1), the coral data do not provide an estimate for SSS, and the TA-DIC and TA-SSS relationships are equally significant. While these relationships are likely to be more complex on a reef system, this study focuses on reconstructing open ocean conditions from a coral shown to closely reflect open ocean water environments [e.g., *Goodkin et al.*, 2012].

3.4. $\delta^{11}B$ to pH Conversion

Conversion of $\delta^{11}B$ to pH was performed three ways for the calibration period of November 1983 to October 1997, excluding the coral sample from November 1993 to October 1995 as too much sample was lost during cleaning to yield a reliable $\delta^{11}B$ measurement.

The first method used the theoretical relationship that $\delta^{11}B$ can be converted to pH by the following equation:

$$pH_{calc} = pK_B - \log\left(\frac{\delta^{11}B_{sw} - \delta^{11}B_{coral}}{\delta^{11}B_{sw} - \alpha \times \delta^{11}B_{coral} - (\alpha - 1) \times 10^3}\right) \quad (2)$$

where $\alpha = 1.0272$ [*Klochko et al.*, 2006] and $pK_B = 8.609$, calculated as a function of average temperature (296.5 K) and salinity (36.6‰) over the instrumental period from November 1983 to October 1997. The second approach substituted a low α value of 1.020 into equation (2) in an attempt to compensate for the offset between seawater and the coral calcification site pH due to up-regulation as previously described. Finally, we investigated a Type I regression of measured coral $\delta^{11}B$ versus seawater pH.

3.5. Calculation of Seawater Parameters and Statistical Analysis

Four main factors control surface ocean pH including (1) atmospheric pCO_2 (partial pressure of CO_2), (2) sea surface temperature, (3) physical water mass transport (e.g., lateral advection or vertical mixing), and (4) biological processes (e.g., primary production). In order to isolate the dominant factors, we investigate expected surface ocean pH changes relative to individual factors using a standard seawater CO_2-carbonate chemistry thermodynamics model, CO2SYS [*Lewis and Wallace*, 1998].

First, a record of surface water pH due to changes in atmospheric CO_2 was calculated at the same time resolution as the coral using CO_2 measurements from the Law Dome Ice Core [*Etheridge et al.*, 1996], the average BATS SSS, SST, and TA, assuming that surface water pCO_2 variations track atmospheric CO_2 on time scales that are rapid (~1 year). Second, average TA, DIC, and SSS from the BATS time series were used with a coral-generated record of SST from 1783 to 1996 [*Goodkin et al.*, 2008b] to generate a record of variations in pH due solely to SST. Finally, a record of pH due to changes in ocean circulation and biogeochemical systems was calculated via the following steps. The coral SST record, average BATS SSS and TA, and the coral pH record were used to calculate a record of DIC. A temporally varying TA record was then calculated from DIC using the observed TA-DIC regression at the same resolution as the coral data (equation (1)). A new record of TA was then used iteratively to recalculate DIC and TA until the procedure converged on a solution for both DIC and TA. A final pH record due to ocean circulation and biogeochemistry was generated using average BATS SSS and SST, and calculated TA and DIC.

Power spectral analysis of the $\delta^{11}B$-generated pH record was performed from 1775 to 1994. The record was prewhitened by removing the mean, and the record was padded to the nearest power of 2. Power spectral analysis using Welch's method was performed using 32 samples (or ¼ of the length) with 50% overlap and plotted in log-log form.

Band-pass filters were applied to the pH record and to 2 year binned climate indices of the SOI, AMO, and NAO to isolate three frequency bands, >24 years, 12–24 years, and 4–8 years. Frequency-specific records were generated using box window band-pass filters selecting for frequencies of 4–8 years and 12–24 years. For the >24 year record, the data were filtered using a 24 year box filter followed by subtraction of a linear fit to the raw data (i.e., lowest frequency filter for each record) to remove the long-term trend.

4. Results

The calculation of pH using the theoretical α (1.0272) applied to the coral $\delta^{11}B$ leads to estimated pH values significantly higher than those measured at BATS (root-mean-square of the residuals, RMSR, and mean bias of 0.38 pH units; supporting information Figure S2a). This finding indicated that the coral likely physiologically increased pH at the site of skeletal growth to facilitate calcificaton. Changing α to 1.0200 overcompensates for this microenvironment effect, producing pHs lower than measured at BATS (RMSR = 0.08 and mean bias of −0.05 pH units) and altering the variability such that boron-generated pH varies approximately 2 times as much as instrumental pH (slope = 2.7, supporting information Figure S2a). Finally, we investigated a simple transformation using a type 1 regression of $\delta^{11}B$ to pH over the calibration period (supporting information Figure S2b)

$$\delta^{11}B = m_0 + m_1 * pH_{instr.} \quad (3)$$

where m_0 is −137.3 pH units, m_1 is 19.8 pH units $‰^{-1}$, $r = 0.61$, $p = 0.19$, and $n = 6$.

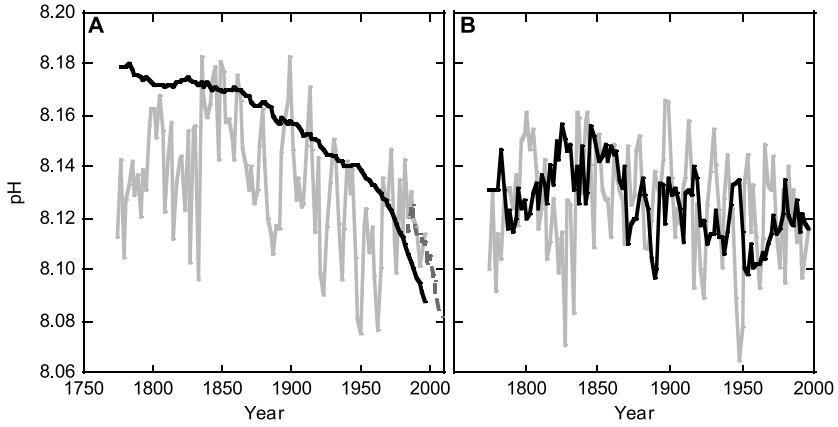

Figure 1. Evaluation of components driving pH variability. (a) Total pH record derived from δ^{11}B of the coral (shaded), pH derived from record of atmospheric pCO_2 reconstructed from the Law Dome ice core (solid), and surface pH from BATS (shaded, dashed). (b) Coral pH record derived solely from SST changes (solid) and coral pH record derived from changes to ocean circulation and biogeochemical seawater changes (shaded).

While the regression encompasses a very narrow range of pH values and thus is not statistically significant ($p > 0.05$), the resulting transformation leads to a more accurate absolute value of pH (RMSR = 0.007 compared to 0.38 pH units for the theoretical) and the same relative variability compared to instrumental pH as is found for the theoretical conversion (standard deviation of both is 0.01 pH units) (supporting information Figure S2c). In comparing the theoretical versus the regression-transformed results, the primary difference is the absolute value rather than the relative variability (supporting information Figure S2d). Therefore, pH records are calculated using equation (3).

Offsets in a coral-derived pH reconstruction are difficult to quantify. The δ^{11}B analytical error converts to pH errors on the order of 0.008 pH units, and the RMSR of the regression in equation (3) provides an error of 0.007 pH units. Both of these errors are of similar magnitude to modern pH measurement errors (~0.003 units), indicating they are not an appropriate approximation of the combined uncertainty. The error on the regression slope, however, is very large due to the limited range of the calibration and is likely unrealistic. In this study, we focus interpretation on relative contributions to and phasing of variability and trends in pH, rather than on absolute pH values. The agreement in variability (slope = 0.9, supporting information Figure S2d) between the thermodynamic conversion (equation (2), $\alpha = 1.0272$) and the instrumental conversion (equation (3)) indicates that this is a valid approach, though does not eliminate potential error in the magnitude of the absolute pH change. However, it is likely that our errors are less than the temporal pH change of up to 0.10 units, and the coherence of low-frequency variables reported later indicates that the reconstructed pH variability is not a white noise process.

The coral δ^{11}B-generated record of pH calculated using equation (3) ranged from a pH of 8.08 to 8.18 with clear oscillatory cycles (Figure 1a). In comparison of the coral pH record to an expected record of surface pH due solely to changes in atmospheric CO_2, the raw coral record on average lies below the atmospherically driven record and exhibits a weaker long-term secular trend. Beyond 1950, the expected ocean pH due to increasing atmospheric CO_2 begins to decline at a faster rate, whereas the coral pH reaches a minimum in 1950 and then increases during the latter part of the twentieth century. The coral record only extends to 1997, and the BATS seawater pH data show a declining trend over the early 21st century. The coral record indicates that factors other than atmospheric pCO_2 also contributed to pH variability in the Sargasso Sea, partially masking any anthropogenic signal (Figure 1a). Note that the relative magnitude of secular trend to decadal variability in the coral pH record is robust to errors in the δ^{11}B-pH slope (equation (3)); errors in the regression slope would only expand/or contract the observed range of variability relative to the atmospheric CO_2 pH signal.

An estimate of pH driven by circulation and biogeochemical (CB) changes showed a similar range of variability to the coral δ^{11}B-derived pH, whereas an SST-derived estimate of pH variations showed half the variability (max-min is 0.10 versus 0.06 pH units and standard deviations are 0.02 and 0.01 pH units, respectively)

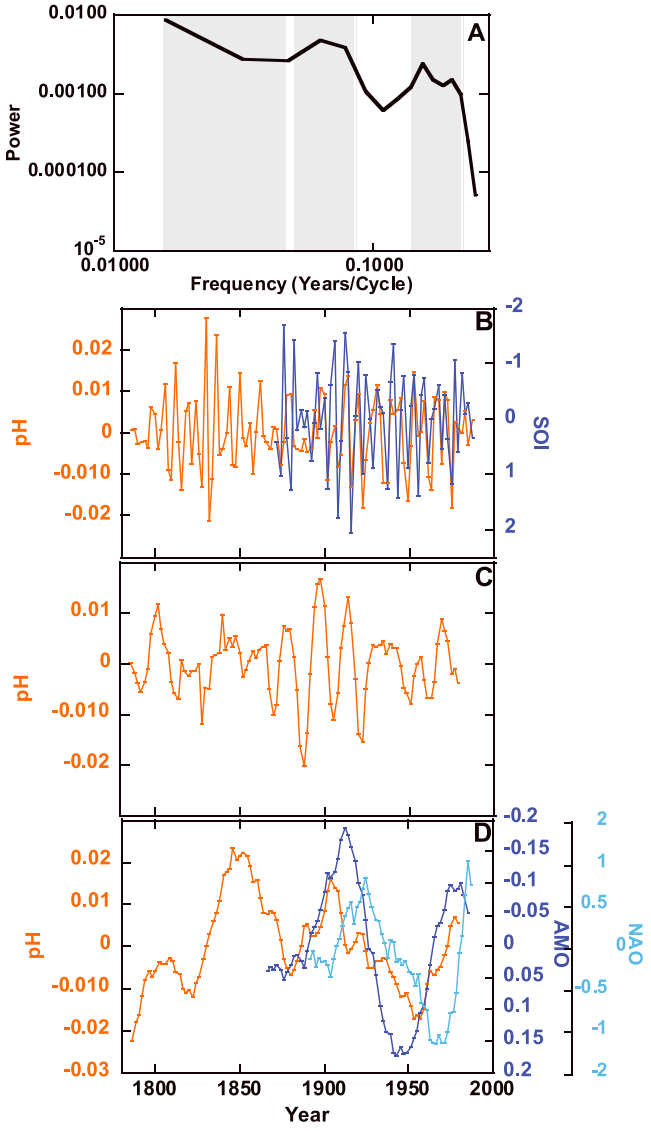

Figure 2. (a) Power spectral analysis of the total Bermuda pH record with frequencies with high power identified (shaded) as 4–8 years per cycle, 12–24 years per cycle, and 24–200 years per cycle. (b) Four to eight year band-pass filtered records of pH (orange) and the Southern Oscillation Index (SOI, blue) versus time. (c) Twelve to 24 year band-pass filtered records of pH (orange). (d) >24 year frequencies of pH (orange) and the AMO (dark blue) and the NAO (light blue).

(Figure 1b). The CB pH variability corresponds to DIC variability of 126 μmol kg^{-1}, with a range of 1976 to 2103 μmol kg^{-1}, assuming DIC and TA covary. The CB- and SST-driven pH records correlate to the coral-derived pH record, $r = 0.82$ and $r = 0.50$, respectively (Figure 1b). Further, subtracting the SST-derived record from the coral-derived record to calculate a nontemperature-derived pH anomaly has a highly significant correlation to the CB record ($r > 0.99$) indicating that circulation and biogeochemistry contributed significantly to Sargasso Sea pH.

Spectral analysis of the coral pH record indicates power in three frequency bands (Figure 2a), 4–8 years per cycle, 12–24 years per cycle, and 24–200 years per cycle. Band-pass filtered records of these frequencies show significant correlations to the SOI ($r = -0.45$ and $p \ll 0.01$) at 4–8 year frequencies and to the AMO ($r = -0.69$, $p \ll 0.0001$) and the NAO ($r = 0.65$, $p << .0001$) at >24 year frequencies (Table 1, Figures 2b–2d). At the >24 year frequency, the correlation to the AMO improves minimally if the AMO leads pH by 4 years ($r = -0.72$, $p \ll 0.0001$), and the correlation to the NAO improves significantly if the NAO lags pH by 8 years ($r = 0.87$, $p \ll 0.0001$). In the 12–24 year band, no climate index is significantly correlated to the coral pH.

5. Discussion

5.1. Atmospheric pCO_2 and SST- Not the Only Drivers of Surface pH

Given the large variability in the overall pH record relative to that attributable to atmospheric CO_2 or SST, changes due to ocean circulation and biogeochemistry (CB) appear to be the dominant mode of influence on seawater pH at Bermuda. The pH changes in the Sargasso Sea due to CB are larger than SST or atmospheric driven changes, even after the Industrial Revolution. The carbon cycle at Bermuda has been tied to large-scale ocean circulation previously [*Bates*, 2012; *Levine et al.*, 2011]. While the pH reconstruction here lacks independent constraints, it clearly shows substantial pH variability not driven by atmospheric CO_2 levels during both preindustrial and postindustrial times. Prior to 1850 and the Industrial Revolution, atmospherically driven pH as expected was relatively constant, whereas the coral pH reconstruction shows variability of up to 0.09 pH units (max-min). Following the onset of the initiation of

Table 1. Correlation (*r*) Values of the Coral pH Records Relative to Climate Indices at Zero Lag and Max Correlation[a]

	SOI		AMO		NAO		
	Zero Lag	Zero Lag	Max Correlation	Lead	Zero Lag	Max Correlation	Lag
4–8 year pH record	*−0.45*	0.16			0.23		
12–24 year pH record	−0.09	0.22			−0.24		
>24 years	NA	*−0.69*	*−0.72*	4 years	*0.65*	*0.87*	8 years

[a]Italicized *r* values are significant ($p < 0.05$). Lead and lag refer to the climate indices relative to the pH record. As the SOI generally occurs on 4 to 7 year frequencies, low-frequency correlations are nonapplicable (NA).

anthropogenic CO_2 emissions from 1850–1950, the atmospherically driven pH record estimates a pH decline of 0.1 units far exceeding the coral pH reconstruction estimate of 0.03 units. After 1950, atmospheric derived pH predicts a further decline of 0.05 pH units whereas the coral records an increase of 0.04 units. While the error in the pH- $\delta^{11}B$ slope could serve to expand or contract the variability in the coral record, the error would not serve to change the secular trends or the decadal variability. From 1950–1996 marks a time when there is a shift in the North Atlantic climate regime (AMO, NAO, etc.), demonstrating that long-term trends are not solely influenced by atmospheric pCO_2.

5.2. Ocean Circulation and Biogeochemical Impacts

At high frequencies (4–8 yr/cycle), coral $\delta^{11}B$-derived pH exhibits a negative correlation with the Southern Oscillation Index at zero lag. This is striking because, although the SOI has a strong teleconnection with tropical Atlantic variability or TAV, it takes 6–10 years for impacts in the tropics to advect to the Sargasso Sea [*Marshall et al*., 2001]. The fact that there is no lag at this time-frequency suggests atmospheric induced changes are driving changes to surface ocean pH surrounding Bermuda. *Alexander et al*. [2001] indicate that the primary impact of a positive (negative) SOI in the Sargasso Sea is in fact a decrease (increase) in SSTs due to an increase (decrease) in heat loss in the region. Although SST is not the primary control of pH changes, surface cooling during a positive ENSO would directly influence the surface water buoyancy and thus the rate of mode water formation and depth of convective mixing [*Billheimer and Talley*, 2013; *Joyce et al*., 2000; *Talley*, 1996]. Both DIC and TA increase with depth while pH simultaneously declines [*Bates et al*., 1996; *Lomas et al*., 2013], indicating that increased convection is leading to a declining surface pH and vice versa.

At midfrequencies (12–24 yr/cycle), seawater pH appears not to be driven by any of the major climate indices impacting the region (Table 1). While overall the most power resides at this frequency (Figure 2a), the power of this frequency band diminishes slightly in the modern day, when instrumental records are available for comparison (Figure 2c).

The lowest frequency pH record (24–200 yr/cycle) has the most significant correlations to climate indices, in agreement with previous research which showed a connection between trace metal concentrations and the NAO hypothesized to result from convective mixing [*Prouty et al*., 2013]. At this frequency, the AMO and the NAO inversely and positively correlate to pH, respectively, with the NAO lagging the pH signal by 8 years at maximum correlation and the AMO leading the pH signal by 4 years (Table 1). At frequencies greater than 10 years, the NAO and the AMO are known to interact. The interaction is most likely due to a shift in the AMO (ocean) altering heat flux from the ocean to the atmosphere, leading to a change in the NAO 6–10 years later [*Gulev et al*., 2013]. At Bermuda, the AMO primarily serves to deliver tropical waters to the subtropics. The AMO interaction is likely masking the decline in surface ocean pH due to the atmosphere exchange as from 1950 to 1996 the AMO weakens, delivering higher pH water from the tropics to the Sargasso Sea (Figure 2d).

6. Conclusion

In conclusion, there are significant ocean circulation and biogeochemical driven changes to surface ocean pH at Bermuda that exceed in magnitude changes due to sea surface temperature and atmospheric pCO_2 over the duration of the 222 year long pH record. From 1950 to 1996, when surface ocean pHs are predicted to decline more rapidly due to anthropogenic CO_2 emissions, pH at Bermuda increases in response to a declining AMO (Figure 2). Instrumental data since 1996 indicate that pH at BATS begins to decline more

steeply after 1996 when there is a relative strengthening of the AMO as can be seen in the subsequent decline of BATS pH (Figure 1a) [*Bates*, 2012; *Enfield et al.*, 2001]. As we evaluate and model predicted changes to surface ocean pH from anthropogenic processes, we must capture how these changes will imprint over natural fluctuations.

Acknowledgments
We are grateful to A. Cohen, S. Smith, and BIOS for sample collection; to P. Martin for the discussion; and to Y.P. Lin and Y.C. Liu for their assistance with sample preparation and analysis. Data are archived at http://www.ncdc.noaa.gov/data-access/paleoclimatology-data. Funding to C.F.Y. was from the Ministry of Education, Taiwan and the NCKU Top University project. Funding to N.F.G. was provided by the University of Hong Kong and the National Research Foundation Singapore under its Singapore NRF Fellowship scheme (National Research Fellow Award NRF-RF2012-03), as administered by the Earth Observatory of Singapore and the Singapore Ministry of Education under the Research Centres of Excellence initiative. S.C.D. and K.A.H. acknowledge support from the National Science Foundation and Woods Hole Oceanographic Institution.

The Editor thanks Christopher Langdon and an anonymous reviewer for their assistance in evaluating this paper.

References

Alexander, I., et al. (2001), New constraints on the origin of the Australian Great Barrier Reef: Results from an international project of deep coring, *Geology*, *29*(6), 483–486.

Anagnostou, E., K. F. Huang, C. F. You, E. L. Sikes, and R. M. Sherrell (2012), Evaluation of boron isotope ratio as a pH proxy in the deep sea coral Desmophyllum dianthus: Evidence of physiological pH adjustment, *Earth Planet. Sci. Lett.*, *349*, 251–260.

Andersson, A. J., K. L. Yeakel, N. R. Bates, and S. de Putron (2014), Future changes in reef metabolism oppose anthropogenic ocean acidification on coral reefs, *Nat. Clim. Change*, *4*, 56–61.

Bates, N. R. (2001), Interannual variability of oceanic CO_2 and biogeochemical properties in the western North Atlantic sub-tropical gyre, *Deep Sea Res., Part II*, *48*, 1507–1528.

Bates, N. R. (2012), Multi-decadal uptake of carbon dioxide into subtropical mode water of the North Atlantic Ocean, *Biogeosciences*, *9*(7), 2649–2659.

Bates, N. R., A. F. Michaels, and A. H. Knap (1996), Seasonal and interannual variability of oceanic carbon dioxide species at the U.S. JGOFS Bermuda Atlantic Time-series study (BATS) site, *Deep Sea Res., Part II*, *43*(2–3), 347–383.

Bates, N. R., A. Amat, and A. J. Anderrsson (2010), The interaction of carbonate chemistry and coral reel calcification: The carbonate chemistry coral reef ecosystem feedback (CREF) hypothesis, *Biogeosciences*, *7*(5), 2509–2530.

Bates, N. R., M. H. P. Best, K. Neely, R. Garley, A. G. Dickson, and R. J. Johnson (2012), Detecting anthropogenic carbon dioxide uptake and ocean acidification in the North Atlantic Ocean, *Biogeosciences*, *9*(7), 2509–2522.

Billheimer, S., and L. Talley (2013), Near cessation of Eighteen Degree Water renewal in the western North Atlantic in the warm winter of 2011–2012, *J. Geophys. Res. Oceans*, *118*, 6838–6853, doi:10.1002/2013JC009024.

Bjerknes, J. (1964), Atlantic air-sea interaction, in *Advanced in Geophysics*, edited by H. E. Landberg and J. Miegham, pp. 1–82, Academic Press, New York.

Doney, S. C., V. J. Fabry, R. Feely, and J. A. Kleypas (2009), Ocean acidification: The other CO_2 problem, *Annu. Rev. Mar. Sci.*, *1*, 169–192.

Enfield, D. B., A. M. Mestas-Nunez, and P. J. Trimble (2001), The Atlantic Multidecadal Oscillation and its relationship to rainfall and river flows in the continental U.S., *Geophys. Res. Lett.*, *28*, 2077–2080, doi:10.1029/2000GL012745.

Etheridge, D. M., L. P. Steele, R. L. Langenfelds, R. J. Francey, J. M. Barnola, and V. I. Morgan (1996), Natural and anthropogenic changes in atmospheric CO_2 over the last 1000 years from air in Antarctic ice and firn, *J. Geophys. Res.*, *101*(D2), 4115–4128, doi:10.1029/95JD03410.

Fung, I. Y., S. C. Doney, K. Lindsay, and J. John (2005), Evolution of carbon sinks in a changing climate, *Proc. Natl. Acad. Sci. U.S.A.*, *102*(32), 11,201–11,206.

Goodkin, N. F., K. A. Hughen, A. L. Cohen, and S. R. Smith (2005), Record of Little Ice Age sea surface temperatures at Bermuda using a growth-dependent calibration of coral Sr/Ca, *Paleoceanography*, *20*, PA4016, doi:10.1029/2005PA001140.

Goodkin, N. F., K. A. Hughen, S. C. Doney, and W. B. Curry (2008a), Increased multidecadal variability of the North Atlantic Oscillation since 1781, *Nat. Geosci.*, *1*(12), 844–848.

Goodkin, N. F., K. A. Hughen, W. B. Curry, S. C. Doney, and D. R. Ostermann (2008b), Sea surface temperature and salinity variability at Bermuda during the end of the Little Ice Age, *Paleoceanography*, *23*, PA3203, doi:10.1029/2007PA001532.

Goodkin, N. F., E. R. M. Druffel, K. A. Hughen, and S. C. Doney (2012), Two centuries of limited variability in subtropical North Atlantic thermocline ventilation, *Nat. Commun.*, *3*, doi:10.1038/ncomms1811.

Gulev, S. K., M. Latif, N. Keenlyside, W. Park, and K. P. Koltermann (2013), North Atlantic Ocean control on surface heat flux on multidecadal timescales, *Nature*, *499*, 464–467.

Hemming, G., and G. N. Hanson (1992), Boron isotopic composition and concentration in modern marine carbonates, *Geochim. Cosmochim. Acta*, *56*, 537–543.

Hönisch, B., N. G. Hemming, A. G. Grottoli, A. Amat, G. N. Hanson, and J. Bijma (2004), Assessing scleractinian corals as recorders for paleo-pH: Empirical calibration and vital effects, *Geochim. Cosmochim. Acta*, *68*(18), 3675–3685.

Hönisch, B., N. G. Hemming, and B. Loose (2007), Comment on "A critical evaluation of the boron isotope-pH proxy: The accuracy of ancient ocean pH estimates" by M. Pagani, D. Lemarchand, A. Spivack and J. Gaillardet, *Geochim. Cosmochim. Acta*, *71*(6), 1636–1641.

Hurrell, J. W. (1995), Decadal trends in the North Atlantic Oscillation: Regional temperatures and precipitation, *Science*, *269*(5224), 676–679.

Hurrell, J. W., Y. Kushnir, G. Ottersen, and M. Visbeck (2003), An overview of the North Atlantic Oscillation, in *The North Atlantic Oscillation: Climatic Significance and Environmental Impact*, edited by J. Hurrell et al., pp. 1–36, AGU, Washington, D. C.

Joyce, T. M., C. Deser, and M. A. Spall (2000), The relation between decadal variability of subtropical mode water and the North Atlantic Oscillation, *J. Clim.*, *13*(14), 2550–2569.

Kaplan, A., M. A. Cane, Y. Kushnir, A. C. Clement, M. B. Blumenthal, and B. Rajagopalan (1998), Analyses of global sea surface temperature 1856–1991, *J. Geophys. Res.*, *103*(C9), 18,567–18,589, doi:10.1029/97JC01736.

Keeling, C. D., R. B. Bacastow, A. E. Bainbridge, C. A. Ekdahl, P. R. Guenther, L. S. Waterman, and J. F. S. Chin (1976), Atmospheric carbon-dioxide variations at Mauna-Loa Observatory, Hawaii, *Tellus*, *28*(6), 538–551.

Klochko, K., A. J. Kaufman, W. S. Yao, R. H. Byrne, and J. A. Tossell (2006), Experimental measurement of boron isotope fractionation in seawater, *Earth Planet. Sci. Lett.*, *248*(1–2), 276–285.

Krief, S., E. J. Hendy, M. Fine, R. Yam, A. Meibom, G. L. Foster, and A. Shemesh (2010), Physiological and isotopic responses of scleractinian corals to ocean acidification, *Geochim. Cosmochim. Acta*, *74*(17), 4988–5001.

Le Quere, C., et al. (2009), Trends in the sources and sinks of carbon dioxide, *Nat. Geosci.*, *2*(12), 831–836.

Levine, N. M., S. C. Doney, I. Lima, R. Wanninkhof, N. R. Bates, and R. A. Feely (2011), The impact of the North Atlantic Oscillation on the uptake and accumulation of anthropogenic CO_2 by North Atlantic Ocean mode waters, *Global Biogeochem. Cycle*, *25*, GB3022, doi:10.1029/2010GB003892.

Lewis, E., and D. W. R. Wallace (1998), Program developed for CO_2 system calculations. ORNL/CDIAC-105, edited, Carbon Dioxide Information Analysis Center, Oak Ridge National Laboratory, U.S. Department of Energy, Oak Ridge, Tennessee.

Lomas, M. W., N. R. Bates, R. J. Johnson, A. H. Knap, D. K. Steinberg, and C. A. Carlson (2013), Two decades and counting: 24-years of sustained open ocean biogeochemical measurements in the Sargasso Sea, *Deep Sea Res., Part II*, *93*, 16–32.

Marshall, J., Y. Kushner, D. Battisti, P. Chang, A. Czaja, R. Dickson, J. Hurrell, M. McCartney, R. Saravanan, and M. Visbeck (2001), North Atlantic climate variability: Phenomena, impacts and mechanisms, *Int. J. Climatol.*, *21*(15), 1863–1898.

McCulloch, M., et al. (2012), Resilience of cold-water scleractinian corals to ocean acidification: Boron isotopic systematics of pH and saturation state up-regulation, *Geochim. Cosmochim. Acta*, *87*, 21–34.

Orr, J. C., et al. (2005), Anthropogenic ocean acidification over the twenty-first century and its impact on calcifying organisms, *Nature*, *437*(7059), 681–686.

Pelejero, C., E. Calvo, M. T. McCulloch, J. F. Marshall, M. K. Gagan, J. M. Lough, and B. N. Opdyke (2005), Preindustrial to modern interdecadal variability in coral reef pH, *Science*, *309*(5744), 2204–2207.

Prouty, N. G., N. F. Goodkin, R. Jones, C. H. Lamborg, C. D. Storlazzi, and K. A. Hughen (2013), Environmental assessment of metal exposure to corals living in Castle Harbour, Bermuda, *Mar. Chem.*, *154*, 55–66.

Quay, P., R. Sonnerup, T. Westby, J. Stutsman, and A. McNichol (2003), Changes in the C-13/C-12 of dissolved inorganic carbon in the ocean as a tracer of anthropogenic CO_2 uptake, *Global Biogeochem. Cycle*, *17*(1), 1004, doi:10.1029/2001GB001817.

Reynaud, S., N. G. Hemming, A. Juillet-Leclerc, and J. P. Gattuso (2004), Effect of pCO_2 and temperature on the boron isotopic composition of the zooxanthellate coral Acropora sp, *Coral Reefs*, *23*(4), 539–546.

Ropelewski, C. F., and P. D. Jones (1987), An extension of the Tahiti-Darwin southern oscillation index, *Mon. Weather Rev.*, *115*, 2161–2165.

Sabine, C. L., et al. (2004), The oceanic sink for anthropogenic CO_2, *Science*, *305*(5682), 367–371.

Talley, L. D. (1996), North Atlantic circulation and variability, reviewed for the CNLS conference, *Physica D*, *98*, 625–646.

Trenberth, K. E. (1984), Signal versus noise in the Southern Oscillation, *Mon. Weather Rev.*, *112*, 326–332.

Trenberth, K. E., and T. J. Hoar (1996), The 1990–1995 El Nino-Southern Oscillation event longest on record, *Geophys. Res. Lett.*, *23*, 57–60, doi:10.1029/95GL03602.

Visbeck, M., H. Cullen, G. Krahmann, and N. Naik (1998), An oceans model's response to North Atlantic Oscillation like wind forcing, *Geophys. Res. Lett.*, *25*, 4521–4524, doi:10.1029/1998GL900162.

Wang, B. S., C. F. You, K. F. Huang, S. F. Wu, S. K. Aggarwal, C. H. Chung, and P. Y. Lin (2010), Direct separation of boron from Na- and Ca-rich matrices by sublimation for stable isotope measurement by MC-ICP-MS, *Talanta*, *82*(4), 1378–1384.